

# Generalized Chaplygin gas model: Cosmological consequences and statefinder diagnosis

M. Malekjani, A. Khodam-Mohammadi and N. Nazari-pooya

**Abstract** The generalized Chaplygin gas (GCG) model in spatially flat universe is investigated. The cosmological consequences led by GCG model including the evolution of EoS parameter, deceleration parameter and dimensionless Hubble parameter are calculated. We show that the GCG model behaves as a general quintessence model. The GCG model can also represent the pressureless CDM model at the early time and cosmological constant model at the late time. The dependency of transition from decelerated expansion to accelerated expansion on the parameters of model is investigated. The statefinder parameters  $r$  and  $s$  in this model are derived and the evolutionary trajectories in  $s-r$  plane are plotted. Finally, based on current observational data, we plot the evolutionary trajectories in  $s-r$  and  $q-r$  planes for best fit values of the parameters of GCG model. It has been shown that although, there are similarities between GCG model and other forms of chaplygin gas in statefinder plane, but the distance of this model from the  $\Lambda$ CDM fixed point in  $s-r$  diagram is shorter compare with standard chaplygin gas model.

**Keywords** Dark energy, Generalized Chaplygin gas model, Statefinder diagnosis

## 1 Introduction

Since 1998, the type Ia supernova (SNe Ia) observations have shown that the universe has undergone to

the accelerating expansion phase (Riess et al., 1999; Perlmutter et al., 1999). This fact has also been supported by many additional observations, including the anisotropy measurements of Cosmic Microwave Background (CMB) from Wilkinson Microwave Anisotropy Probe (WMAP) (Spergel et al., 2003, 2007), the data of Large Scale Structure of universe (LSS) from Sloan Digital Sky Survey (SDSS) (Tegmark et al., 2004a,b) and X-ray experiments (Allen et al., 2004). The current accelerating expansion of universe indicates that in addition to the existence of dark matter, which is required to explain the galactic dynamics and the formation of structures (Bosma, 1981), the universe is dominated by an exotic energy component with negative pressure, dubbed the dark energy. In another word, in the framework of standard cosmology, the dark energy (DE) scenario is a theoretical solution to explain the accelerating expansion of the universe. The combined analysis of cosmological observations suggest that the universe consists of about 70% dark energy, 30% dust matter (cold dark matter plus baryons), and negligible radiation. The cosmological constant, whose equation of state is independent of cosmic time, is a simple solution of DE problem. However, it suffers from two well known problems, namely, the fine-tuning and the cosmic coincidence problems (Copeland, Sami & Tsujikawa, 2006). In addition to cosmological constant, many kinds of dynamical DE models, whose equation of state is no longer a constant but slightly evolves with time, have been suggested to interpret the cosmic acceleration. The quintessence (Wetterich, 1988), phantom field (Caldwell, 2002), quintom (Elizalde, Nojiri & Odinstov, 2004), Chaplygin gas models (Kamenshchik, Moschella & Pasquier, 2001), K-essence (Chiba, Okabe & Yamaguchi, 2000), tachyon field (Sen, 2002), holographic (Cohen, Kaplan & Nelson, 1999) and agegraphic (Cai, 2007) DE models are the examples of dynamical DE model. It is emphasized that

---

M. Malekjani, A. Khodam-Mohammadi and N. Nazari-pooya  
Department of Physics, Faculty of Science, Bu-Ali Sina University, Hamedan 65178, Iran.

malekjani@basu.ac.ir.  
khodam@basu.ac.ir.  
nazari@basu.ac.ir.

the predictions of cosmological constant model is still fitted to the observation (Jassal, Bagla & Padmanabhan, 2004). Therefore, a suggested dynamical DE model should not be faraway from cosmological constant. Besides the DE models, modified gravity theories such as scalar tensor cosmology (Boisseau et al., 2000), braneworld models (Dvali, Gabadadze & Porrati, 2008) have been suggested to solve the accelerated expansion of universe.

The Chaplygin gas is one of the candidate of DE models to explain the accelerated expansion of the universe. The striking features of Chaplygin gas DE is that it can be assumed as a possible unification of dark matter and DE. The Chaplygin gas plays a dual role at different epoch of the history of the universe: it can be as a dust-like matter in the early time, and as a cosmological constant at the late time. This model from the field theory points of view has been investigated in (Bilic, Tupper & Viollier, 2002). The Chaplygin gas emerges as an effective fluid associated with D-branes (Bordemann & Hoppe, 1993) and can also be obtained from the Born-Infeld action (Bento, Bertolami & Sen, 2004). The simplest form of Chaplygin gas model called standard Chaplygin gas (SCG) which has been used to explain the accelerated expansion of universe (Gori, 2004). Although the SCG model can interpret the accelerated expansion of universe, but it can not explain the astrophysical problems such as the structure formation and cosmological perturbation power spectrum (Sandvik, 2004). Subsequently, the SCG is extended into the generalized Chaplygin gas (GCG) which could construct viable cosmological models. Same as SCG model, the GCG model can obtain the accelerated expansion of the universe (Setare, 2007).

The quantities  $H = \dot{a}/a$  and  $q = -\ddot{a}/aH^2$ , namely, the Hubble parameter and the deceleration parameter, are the geometrical parameters to describe the expansion history of universe, where  $a$  is the scale factor and dot denotes the derivative with respect to time. It is obvious that  $\dot{a} > 0 (H > 0)$  indicates the expansion of universe and  $\ddot{a} > 0 (q < 0)$  means that the universe is undergoing an accelerated expansion. The various DE models give the same value of  $q_0$  at present time, therefore, the hubble parameter  $H$  (first time derivative of scale factor) and the deceleration parameter  $q$  (second time derivative of scale factor) can not discriminate the various DE models. For this aim, we need the higher order of time derivative of scale factor. Using the third order time derivative, Sahni, et al. (Sahni et al., 2003) and Alam et al. (Alam et al., 2003a) introduced the statefinder pair  $\{r,s\}$  in order to remove the degeneracy of  $H_0$  and  $q_0$  of different DE models. The

statefinder pair  $\{r,s\}$  is defined as

$$r = \frac{\ddot{a}}{aH^3}, \quad s = \frac{r-1}{3(q-1/2)}, \quad (1)$$

It is clear that the statefinder is a geometrical diagnostic, because it depends only on the scale factor. The role of statefinder pair is to distinguish the behaviors of cosmological evolution of dark energy models with the same values of  $H_0$  and  $q_0$  at the present time. Up to now, the statefinder diagnostic tool has been used to study the various dark energy models. The various DE models have different evolutionary trajectories in  $\{r,s\}$  plane, therefore the statefinder is a good tool to discriminate DE models. For example, the well-known  $\Lambda$ CDM model corresponds to a fixed point  $\{r=1, s=0\}$  in  $\{r,s\}$  plane (Sahni et al., 2003). Also, the quintessence DE model (Sahni et al., 2003; Alam et al., 2003b), the interacting quintessence models (Zimdahl & Pavon, 2004; Zhang, 2005a), the holographic dark energy models (Zhang, 2005b; Zhang et al., 2007), the holographic dark energy model in non-flat universe (Setare, J. Zhang & X. Zhang, 2007), the phantom model (Chang et al., 2007), the tachyon (Shao & Gui, 2007), the agegraphic DE model with and without interaction in flat and non-flat universe (Wei & Cai, 2007; Malekjani & Khodam-Mohammadi, 2010) and the interacting new agegraphic DE model in flat and non-flat universe (Zhang et al., 2010; Khodam-Mohammadi & Malekjani et al., 2010), are analyzed through the statefinder diagnostic tool. The SCG model is analyzed in terms of statefinder with or without dust component (Gorini, Kamenshchik & Moschella, 2003). In 2003, the generalized cosmic chaplygin gas (GCCG) model is introduced by Gonzalez-Diaz (Gonzalez-Diaz, 2003). The interesting features of GCCG model is that it can be stable and free from un physical behaviors even when the vacuum fluid satisfies the phantom energy condition (Gonzalez-Diaz, 2003). Chakraborty, et al. (2007) have performed the statefinder analysis for GCCG model and for particular choice of interaction parameter, they have shown the role of statefinder parameters for the evolution of the universe (Chakraborty et al., 2007). Zhang, et al., (2006) proposed a new model to describe the unification of dark matter and DE, namely the new generalized chaplygin gas (NGCG) model and calculated the cosmological consequences and statefinder analysis for this model. The advantage of NGCG model is that it can represent the other forms of dark energy models such as quintessence-like and phantom-like dark energy (X. Zhang, We & J. Zhang, 2006). In this paper, first we study the cosmological consequences of GCG model, and then examine it by

means of statefinder diagnostic tool. Here, we also study the dependency of the cosmological quantities and statefinder diagnostic on the parameters of GCG model. The paper is organized as follows: In section 2, we introduce the GCG model and derive the statefinder parameters  $\{r,s\}$  for this model. In section 3, the numerical results are presented. We conclude in section 4.

## 2 GCG model

The equation of state of GCG is given by

$$p = -\frac{A}{\rho^\alpha} \quad (2)$$

where  $A > 0$  and  $\alpha \geq 0$  are the parameters of the model (Bento, Bertolami & Sen, 2002). In the case of  $\alpha = 1$ , the GCG model is reduced to SCG model. Also, for  $\alpha = 0$  it can be reduced to standard  $\Lambda$ CDM model. In the framework of Friedmann- Robertson-Walker (FRW) cosmology, using Eq. (2) and the conservation equation  $d(\rho a^3) = -pd(a^3)$ , the energy density of GCG is written as

$$\rho_{GCG} = \rho_{0GCG}[A_s + (1 - A_s)a^{-3(1+\alpha)}]^{\frac{1}{1+\alpha}}, \quad (3)$$

where  $a$  is the scale factor,  $A_s = A/\rho_{0GCG}^{1+\alpha}$  and  $\rho_{0GCG}$  is the present value of energy density. Using Eq. (2) and (3), the equation of state (EoS) parameter of GCG model can be obtained as

$$w_{GCG} = -\frac{A_s a^{3(1+\alpha)}}{1 - A_s + A_s a^{3(1+\alpha)}} \quad (4)$$

From Eq. (4), it is clear to show that at the early time ( $a \rightarrow 0$ ), the EoS parameter tends to zero ( $w_{GCG} \rightarrow 0$ ) and at the late time ( $a \rightarrow \infty$ ):  $w_{GCG} \rightarrow -1$ , which are equal to the EoS parameter of matter and cosmological constant, respectively. Therefore, the EoS parameter of GCG model is constrained to the interval  $-1 \leq w_\Lambda \leq 0$  and can be viewed as a general quintessence DE model. Moreover, Eq. (4) shows that at the early time the GCG fluid can be interpreted as a CDM ( $w_{GCG} \rightarrow 0$ ), and at the late time it mimics the  $\Lambda$ CDM model ( $w_{GCG} \rightarrow -1$ ). We can also see that for  $A_s > 1$  the EoS parameter  $w_{GCG} < -1$  and the GCG model can cross the phantom divide.

Since the dark matter and dark energy are unified by GCG model, therefore it can be de-composited into two components of dark matter and dark energy, as  $\rho_{GCG} = \rho_{de} + \rho_{dm}$ . Also, by assuming the pressureless CDM, we have  $p_{GCG} = p_{de}$ . Considering the evolving density of CDM as

$$\rho_{dm} = \rho_{0dm}a^{-3}, \quad (5)$$

it is obvious that the energy density of DE in GCG model can be derived as

$$\begin{aligned} \rho_{de} &= \rho_{GCG} - \rho_{dm} = \\ &\rho_{0GCG}[A_s + (1 - A_s)a^{-3(1+\alpha)}]^{\frac{1}{1+\alpha}} - \rho_{0dm}a^{-3}. \end{aligned} \quad (6)$$

By assuming that the universe is filled by GCG component (DE+CDM) and baryonic matter component, the total energy density is  $\rho_t = \rho_{GCG} + \rho_b$ . In the case of flat universe, the friedmann equation for GCG model is written as

$$\begin{aligned} H^2 &= \frac{8\pi G}{3}\rho_t \\ &= \frac{8\pi G}{3}\left(\rho_{0GCG}[A_s + (1 - A_s)a^{-3(1+\alpha)}]^{\frac{1}{1+\alpha}} + \rho_{0b}a^{-3}\right) \end{aligned} \quad (7)$$

where  $\rho_{0b}$  is the present density of baryonic matter. Substituting the dimensionless parameters

$$\begin{aligned} \rho_{0GCG} &= \frac{3H_0^2}{8\pi G}\Omega_{GCG} \\ \rho_{0b} &= \frac{3H_0^2}{8\pi G}\Omega_b \\ \Omega_{GCG} + \Omega_b &= 1, \end{aligned} \quad (8)$$

in Eq. (7), the Hubble parameter is expressed as

$$\begin{aligned} H^2 &= H_0^2 E^2(a) = \\ &H_0^2 \left( (1 - \Omega_b)[A_s + (1 - A_s)a^{-3(1+\alpha)}]^{\frac{1}{1+\alpha}} + \Omega_b a^{-3} \right), \end{aligned} \quad (9)$$

where  $E(a)$ , the the normalized Hubble parameter, is defined as

$$E(a) = \left( (1 - \Omega_b)[A_s + (1 - A_s)a^{-3(1+\alpha)}]^{\frac{1}{1+\alpha}} + \Omega_b a^{-3} \right)^{1/2} \quad (10)$$

Recently, Xu and Lu (Xu & Lu, 2010), by applying the Markov Chain Monte Carlo approach on the latest observational data, have constrained the GCG model. The observational data that have been used are: the constitution dataset (Hicken, 2009) including 397 type supernova Ia (SNIa), the observational Hubble data (OHD) (Simon, 2005), the cluster X-ray gas mass fraction (Allen et al., 2008), the measurement results of baryon acoustic oscillation (BAO) from Sloan Digital Sky Survey (SDSS) (Eisenstein, 2005) and Two Degree Field Galaxy Redshift Survey (2dFGRS) (Percival, 2009), and the cosmic microwave background (CMB) data from five-year WMAP (Komatsu, 2009). They obtained that in the flat universe, the best fit values of the GCG model parameters ( $A_s, \alpha$ ) and the cosmological parameters ( $\Omega_b h^2, H_0$ ) with their confidence level are:  $A_s = 0.76_{-0.039}^{+0.029}$  ( $1\sigma$ )  $_{-0.046}^{+0.034}$  ( $2\sigma$ ),  $\alpha = 0.033_{-0.071}^{+0.066}$

$(1\sigma)_{-0.087}^{+0.096}$  ( $2\sigma$ ),  $\Omega_b h^2 = 0.0233_{-0.0016}^{+0.0023}$  ( $1\sigma$ )  $_{-0.0020}^{+0.0029}$  ( $2\sigma$ ) and  $H_0 = 69.97_{-2.78}^{+2.87}$  ( $1\sigma$ )  $_{-3.08}^{+3.48}$  ( $2\sigma$ ), with minimum chi-square  $\chi_{min}^2 = 519.342$ . At following, we derive the deceleration parameter  $q$  and the statefinder pair  $\{r, s\}$  for GCG model.

The deceleration parameter  $q$ , which denotes the expansion phase of the universe, is given by

$$q = -\frac{\ddot{H}}{H^2} - 1 \quad (11)$$

Re-witting  $q$  in terms of  $E$ , we have

$$q(x) = -\frac{1}{E} \frac{dE}{d \ln a} - 1 \quad (12)$$

Substituting  $E$  from Eq. (10) in (12), we obtain the deceleration parameter  $q$  for GCG model as

$$\begin{aligned} q &= \left[ 3(1 - \Omega_b) \left( A_s + (1 - A_s) a^{-3(1+\alpha)} \right)^{-\frac{\alpha}{1+\alpha}} \right. \\ &\quad \left. \times (1 - A_s) a^{-3(1+\alpha)} + 3\Omega_b a^{-3} \right] / \\ &\quad \left[ 2(1 - \Omega_b) \left( A_s + (1 - A_s) a^{-3(1+\alpha)} \right)^{\frac{1}{1+\alpha}} \right. \\ &\quad \left. + 2\Omega_b a^{-3} \right] - 1. \end{aligned} \quad (13)$$

Eq. (13) explicitly shows the dependence of deceleration parameter  $q$  on the GCG model parameter  $A_s$  and  $\alpha$ . Now, we derive the statefinder pair  $\{r, s\}$  for GCG model. Using the definition of statfinder parameters in Eq. (1), we have

$$r = \frac{\ddot{a}}{aH^3} = \frac{\ddot{H}}{H^3} - 3q - 2. \quad (14)$$

Similar to  $q$ , the parameter  $r$  can be re-written in terms of  $E$  as

$$r = \frac{1}{E} \frac{d^2 E}{d(\ln a)^2} + \frac{1}{E^2} \left( \frac{dE}{d \ln a} \right)^2 + \frac{3}{E} \frac{dE}{d \ln a} + 1, \quad (15)$$

also the parameter  $s$  can be obtained as

$$s = -\frac{\frac{1}{E} \frac{d^2 E}{d(\ln a)^2} + \frac{1}{E^2} \left( \frac{dE}{d \ln a} \right)^2 + \frac{3}{E} \frac{dE}{d \ln a}}{\frac{3}{E} \frac{dE}{d \ln a} + \frac{9}{2}} \quad (16)$$

Substituting  $E$  from Eq. (10) in (15) and (16), we obtain  $r$  and  $s$  for GCG model as

$$\begin{aligned} r &= 1 + \left[ 9(1 - \Omega_b)(1 - A_s) \times \right. \\ &\quad \left. \left( A_s + (1 - A_s) a^{-3(1+\alpha)} \right)^{-\frac{1+2\alpha}{1+\alpha}} A_s \alpha a^{-3(1+\alpha)} \right] / \\ &\quad \left[ 2(1 - \Omega_b) \left( A_s + (1 - A_s) a^{-3(1+\alpha)} \right)^{\frac{1}{1+\alpha}} + 2\Omega_b a^{-3} \right], \end{aligned} \quad (17)$$

$$s = -\frac{(1 - A_s) \alpha a^{-3(1+\alpha)}}{A_s + (1 - A_s) a^{-3(1+\alpha)}} \quad (18)$$

For  $\alpha = 0$  or  $A_s = 1$ , we obtain  $\{r = 1, s = 0\}$  which refers to the statefinder pair of spatially flat  $\Lambda$ CDM model. Departure of a given dark energy model from the fixed point  $\{r = 1, s = 0\}$  is a criterion for evaluating of this model from spatially flat  $\Lambda$ CDM model (Sahni et al., 2003). The importance of the statefinder diagnostic is that the current values of the parameters  $s$  and  $r$  can be extracted from the observational data of SNAP (Super Nova Acceleration Probe) type experiments. Therefore, the statefinder diagnostic combined with the future SNAP observation can help us to discriminate between different dark energy models.

### 3 Numerical results

In this section we discuss the cosmological consequences led by GCG model. For this aim, the evolution of EoS parameter of GCG model,  $w_{GCG}$ , the deceleration parameter  $q$  and cosmological evolution of dimensionless hubble parameter  $E$ , are studied. Then we study the GCG model by means of statefinder diagnostic point of view.

#### 3.1 EoS parameter

Solving Eq. (4), the evolution of  $w_{GCG}$  as a function of scale factor for different model parameters  $A_s$  and  $\alpha$  is shown in Fig. (1). In upper panel, by fixing  $A_s = 0.76$  based on observational constrain, we vary the parameter  $\alpha$  as 1, 0.1, 0.01. For  $a < 1$ , increasing the parameter  $\alpha$  leads to a larger value of  $w_{GCG}$ . While, at  $a > 1$ ,  $w_{GCG}$  is smaller for larger value of  $\alpha$ . Here, we see the dual role of GCG model at different epoch of the history of universe: It can be assumed as a pressureless dark matter ( $w = 0.0$ ) at the early time and a cosmological constant with  $w = -1$  at the late time. In lower panel, by fixing  $\alpha = 0.033$  based on observational constrain, we plot  $w_{GCG}$  for different illustrative values of  $A_s$ . For  $A_s = 0.0$ , we see that  $w_{GCG} = 0.0$ , which refers to the pressureless CDM model. In the case of  $A_s = 1.0$ , we have  $w_{GCG} = -1$ , which denotes the cosmological constant. For  $0 < A_s < 1$ , we can see  $-1 < w_{GCG} < 0$ , denoting the time varying equation of state of GCG model and representing the general quintessence behavior of this model. Also, increasing the parameter  $A_s$  leads to smaller value of  $w_{GCG}$ .

### 3.2 Deceleration parameter

Here we calculate the evolution of deceleration parameter,  $q$  for a universe dominated by GCG model and investigate the dependency of  $q$  on the parameters of model. In Fig.(2), by solving Eq.(13), the evolution of  $q$  as a function of scale factor for different illustrative values of model parameters  $\alpha$  and  $A_s$  is calculated. Here we adopt the observational value of  $\Omega_b h^2$  as 0.0233. First we fix the parameter  $A_s$  as 0.76 and vary the parameter  $\alpha$  as 1.0, 0.1 and 0.01 (upper panel). Then, by fixing  $\alpha = 0.033$ , we choose the illustrative values for  $A_s$  as 0.0, 0.1, 0.2, 0.3 and 1.0 (lower panel). In upper panel, one can see that by increasing the parameter  $\alpha$   $q$  becomes larger for  $a < 1$  and smaller for  $a > 1$ . The transition from decelerated expansion ( $q > 0$ ) to accelerated expansion ( $q < 0$ ) takes place earlier for smaller value of  $\alpha$ . From this figure we see that  $q = 1/2$  at the early time (CDM dominated universe) and  $q$  tends to  $-1$  at the late time ( $\Lambda$ CDM dominated universe). This fact can also be seen in the lower panel for any value of  $A_s$  in the interval  $0 < A_s < 1$ . For  $A_s = 0.0$ , we have the constant deceleration parameter  $q = 1/2$ , corresponding to the CDM dominated universe. For the values in the interval  $0 < A_s < 1$ ,  $q$  starts from  $1/2$  at the early time and leads to  $-1$  at the late time. Furthermore,  $q$  becomes larger for lower values of  $A_s$ . Transition from decelerated expansion ( $q > 0$ ) to accelerated expansion ( $q < 0$ ) occurs sooner for higher values of  $A_s$ .

### 3.3 Hubble parameter

At following, we study the Hubble parameter which evaluates the expansion rate of the universe for GCG cosmology. Using Eq. (10), we plot the cosmological evolution of  $E(a)$  in Fig. (3). First, we fix the coefficient  $A_s = 0.76$  and vary the model parameter  $\alpha$  as 1.0, 0.1 and 0.01 (see upper panel). In this case, we see that the larger value the parameter  $\alpha$  is taken, the bigger value the Hubble expansion rate  $E(a)$  gets. In lower panel, by fixing  $\alpha$ , we vary the coefficient  $A_s$  as 0.0, 0.1, 0.2, 0.3 and 1.0. The case of  $A_s = 1.0$  represents the standard  $\Lambda$ CDM model and  $A_s = 0.0$  denotes the CDM model. Here, one can see that for larger value of  $A_s$ , the Hubble expansion rate  $E(a)$  becomes smaller at  $a < 1$  and larger at  $a > 1$ . Therefore, from the above analysis, we find that both parameters  $A_s$  and  $\alpha$  can impact the cosmic expansion history in GCG model.

### 3.4 Statefinder parameters

The statefinder pair  $\{r,s\}$  for GCG model is given by Eqs. (17) and (18), respectively. In statefinder plane,

the horizontal axis is defined by the parameter  $s$  and vertical axis by the parameter  $r$ . In this diagram, the standard  $\Lambda$ CDM model corresponds to a fixed point  $\{r = 1, s = 0\}$ . At the early time,  $a \rightarrow 0$ , the statefinder pair  $\{r, s\}$  defined in Eqs. (17) and (18) are reduced as follows:

$$r = \frac{9(1 - \Omega_b)(1 - A_s)^{-\frac{1+2\alpha}{1+\alpha}} A_s \alpha \alpha^{3(\alpha+1)}}{2(1 - \Omega_b)(1 - A_s)^{\frac{1}{1+\alpha}}} + 1, \quad s = -\alpha, \quad (19)$$

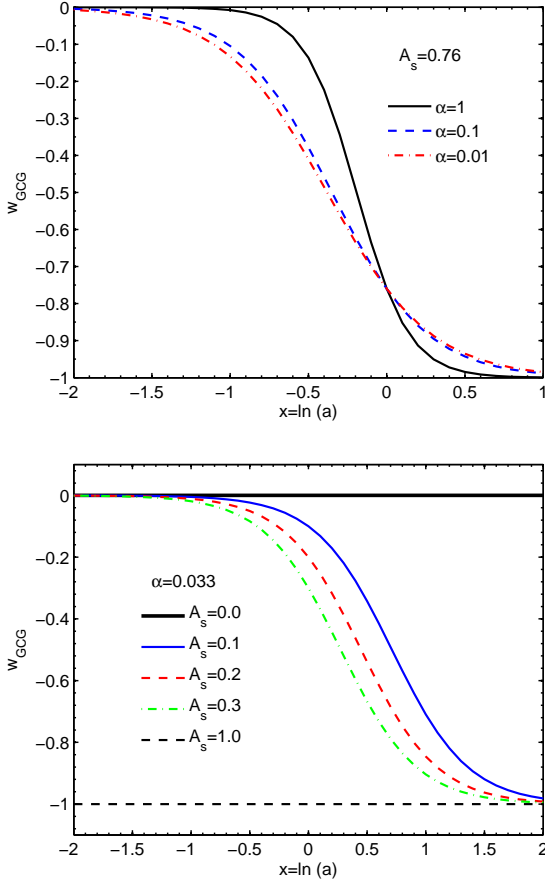
therefore we see that at the early time,  $a \rightarrow 0$ , the statefinder pair  $\{r,s\}$  for GCG model are:  $\{s = -\alpha, r = 1\}$ . From Eqs. (17) and (18), we can also obtain the statefinder pair  $\{r,s\}$  at the late time,  $a \rightarrow \infty$ , as  $\{r = 1, s = 0.0\}$ . Hence, the GCG model mimics the cosmological constant at the late time. In Fig.(4), we show the evolutionary trajectories of GCG model in statefinder plane. In upper panel, by fixing  $A_s = 0.76$ , we choose the illustrative values 0.1, 0.2 and 0.3 for  $\alpha$ . While the universe expands, the trajectories of the statefinder start from the fixed point  $\{s = -\alpha, r = 1\}$  at the early time. The parameter  $r$  starts to increase and then decays, while the parameter  $s$  increases from the initial value  $s = -\alpha$  at the early time to  $s = 0.0$  at the late time. Here, we can easily see that the statefinder trajectory is dependent on the parameter  $\alpha$  of GCG model. Different values of  $\alpha$  give the different evolutionary trajectories in  $\{s, r\}$  plane. The colored points on the curves represent the today's values of statefinder parameters  $(s_0, r_0)$  and the star symbol indicates the standard  $\Lambda$ CDM model. The distance to  $\Lambda$ CDM fixed point becomes shorter for smaller value of  $\alpha$ . We can also see that for smaller values of  $\alpha$ , the parameter  $s$  increases and the parameter  $r$  decreases. In lower panel, by fixing  $\alpha = 0.033$ , we plot the evolutionary trajectories in  $s - r$  diagram for different values of the parameter  $A_s$ . From Eqs. (17) and (18), we have  $\{r = 1, s = -\alpha\}$  for  $A_s = 0.0$ . Therefore, for  $A_s = 0.0$  we have a fixed point  $\{s = -\alpha, r = 1\}$  in  $s - r$  plane. Also from Eqs. (17) and (18) one can see that  $\{s = 0, r = 1\}$  for  $A_s = 1.0$ . Hence, in the case of  $A_s = 1.0$ , the statefinder parameters  $\{s, r\}$  are coincide to the  $\Lambda$ CDM fixed point in  $s - r$  plane. For different values of  $A_s$  in the interval  $0 < A_s < 1$ , we have the different evolutionary trajectories in  $s - r$  plane (see the right panel). Therefore, the parameter  $A_s$  affects the evolutionary trajectories in  $s - r$  plane. The distance to  $\Lambda$ CDM fixed point  $\{s = 0.0, r = 1.0\}$  becomes shorter for larger values of  $A_s$ . The colored points represent the today's values of the parameters  $(s_0, r_0)$  for different values of  $A_s$ . Here, we see that the parameter  $s_0$  increases for larger values of  $A_s$  and the parameter  $r_0$  is largest for  $r = 0.5$ . In

Fig. (5), we plot the evolutionary trajectory in  $s-r$  plane (upper panel) and  $q-r$  plane (lower panel) for the best fit observational values:  $A_s = 0.76$  and  $\alpha = 0.033$ . In upper panel the evolutionary trajectory starts from  $(s = -0.033, r = 1)$  at the past time, reaches to the  $(s = -0.033, r = 1)$  at the present time (circle point) and ended at  $(s = 0, r = 1)$  at the future. This behavior of GCG model in statefinder plane is similar to NGCG model at the early time (X. Zhang, We & J. Zhang, 2006), where they found that the universe starts from the initial value  $(r = 1, s = -\alpha)$  in  $s-r$  plane. Gorini, et al, (Gorini, Kamenshchik & Moschella, 2003) calculated the trajectory of SCG in  $s-r$  plane and showed that the universe in SCG model starts from  $(s = -1, r = 1)$  reaches to  $(s_0 = -0.3, r = 1.9)$  at the present time and finally mimics the  $\Lambda$ CDM model at the late time. Therefore the distance of  $(s_0, r_0)$  in GCG model constrained by the above observational value from the standard fixed point  $\Lambda$ CDM  $(s = 0, r = 1)$  is shorter compare with SCG model. As a similarity, we see that for both model the universe mimics the  $\Lambda$ CDM model at the late time. Moreover, the behavior of the trajectory in  $s-r$  plane is similar for both model, where by expanding the universe,  $r$  increases to a maximum value then decreases to  $r = 1$  at the late time and the parameter  $s$  increases forever. In lower panel the evolutionary trajectory in  $q-r$  plane starts from  $(q = 0.5, r = 1)$  at the past (note that  $(q = 0.5, r = 1)$  corresponds to the CDM dominated universe), reaches to  $(q = -0.575, r = 1.26)$  at the present time and ended at  $(q = -0.965, r = 1)$  at the future.

#### 4 Conclusion

Summarizing this work, we investigated the generalized Chaplygin gas (GCG) model in spatially flat universe. Here we studied the cosmological consequences of GCG model by calculating the evolution of EoS parameter  $w_{GCG}$ , deceleration parameter  $q$  and cosmological evolution  $E(a)$  of GCG model. In the GCG cosmology, the universe starts from the CDM-dominated phase at the early time to the DE-dominated universe at the late time. The GCG fluid as a general quintessence dark energy model can be viewed as a pressureless matter fluid ( $w_{GCG} = 0.0$ ) at the early time and as a cosmological constant ( $w_{GCG} = -1$ ) at the late time. We also obtained the deceleration parameter  $q$  in GCG model and studied the evolutionary treatment of  $q$  as a function of scale factor in this model. In GCG model, the parameter  $q$  starts from the initial value  $1/2$  at the early time (CDM-dominated universe) and converges to  $-1$  at the late time ( $\Lambda$ -dominated universe). Furthermore,

we exhibit the cosmological evolution of  $E(a)$  (normalized Hubble parameter,  $E(a) = H(a)/H_0$ ). For GCG model, both the parameters  $A_s$  and  $\alpha$  affect the cosmological evolution. Finally, we performed the statefinder diagnostic tool on the GCG model. Since many cosmological models have been proposed to interpret the accelerated expansion of universe, the statefinder diagnostic tool with the parameters  $r$  and  $s$  which are constructed by higher order derivative of the scale factor is needed to discriminate between them. Moreover, the present values of  $r$  and  $s$  can be viewed as a discriminator for testing a given dark energy model if it can be extracted from observational data in a model-independent way. Here we derived the statefinder parameters  $r$  and  $s$  for GCG model and studied the evolutionary trajectories of this model in  $s-r$  plane. The dependence of the evolutionary trajectories and the today's value of  $\{s, r\}$  on the model parameters  $A_s$  and  $\alpha$  has been investigated. The lower value of  $\alpha$  and higher value of  $A_s$  result the shorter distance from standard  $\Lambda$ CDM model in  $s-r$  diagram. Eventually, we plotted the evolutionary trajectory of GCG model in  $s-r$  and  $q-r$  plane based on current observational data and found that the distance of GCG model from the standard  $\Lambda$ CDM model in  $s-r$  plane is shorter compare with SCG model. However, both SCG and GCG models have a similar trajectories in  $s-r$  diagram. Furthermore, the behavior of GCG model in statefinder plane is similar to NGCG model at the early time (X. Zhang, We & J. Zhang, 2006), where the universe expands from the initial value  $(r = 1, s = -\alpha)$  in  $s-r$  plane.



**Fig. 1** The evolution of EoS parameter of GCG model,  $w_{GCG}$ , versus  $x = \ln a$  for different illustrative values of parameters  $A_s$  and  $\alpha$ . In upper panel, fixing  $A_s$  by best fit value:  $A_s = 0.76$ , we vary  $\alpha$  as 1, 0.1, 0.01 corresponding to black solid line, blue dashed line and red dotted-dashed line, respectively. The case of  $\alpha = 1.0$  exhibits the standard Chaplygin gas (SCG) model. In lower panel, fixing  $\alpha$  by best fit value:  $\alpha = 0.033$ ,  $A_s$  is varied as 0 (black thick solid line), 0.1 (blue solid line), 0.2 (red dashed line), 0.3 (green dotted-dashed line) and 1.0 (black dashed line). The cases of  $A_s = 0.0$  and  $A_s = 1.0$  exhibit the EoS parameter of pressureless matter and cosmological constant fluids, respectively.

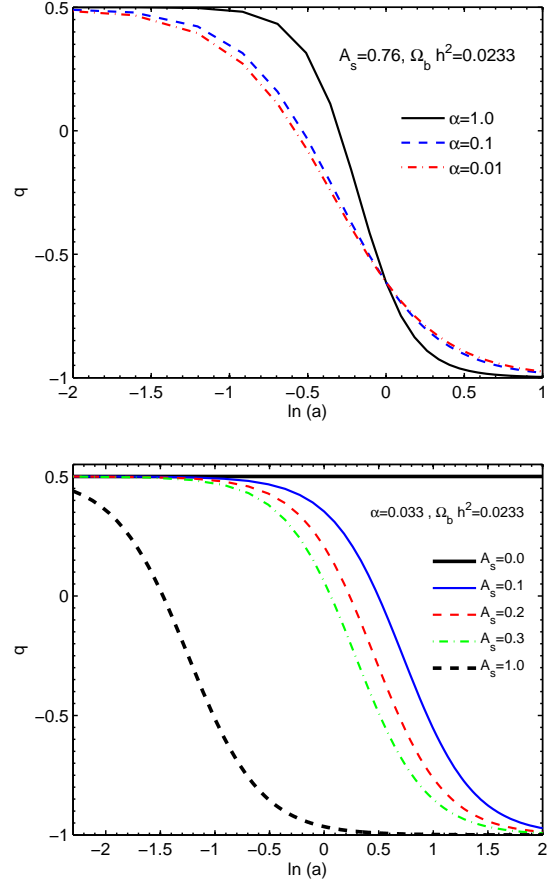


**Fig. 2** The evolution of deceleration parameter  $q$  in GCG model versus  $x = \ln a$  for different illustrative values of model parameters  $A_s$  and  $\alpha$ . In upper panel, by fixing  $A_s = 0.76$ , we vary  $\alpha$  as 0.2, 0.1, 0.01 corresponding to black solid line, blue dashed line and red dotted-dashed line, respectively. The case of  $\alpha = 1.0$  represents the SCG model. In lower panel, by fixing  $\alpha = 0.033$ ,  $A_s$  is varied as 0 (black thick solid line), 0.1 (blue solid line), 0.2 (red dashed line), 0.3 (green dotted-dashed line) and 1. (black thick dashed line). The cases of  $A_s = 0.0$  and  $A_s = 1.0$  represent the evolution of  $q$  in CDM-dominated and  $\Lambda$ -dominated universe, respectively.

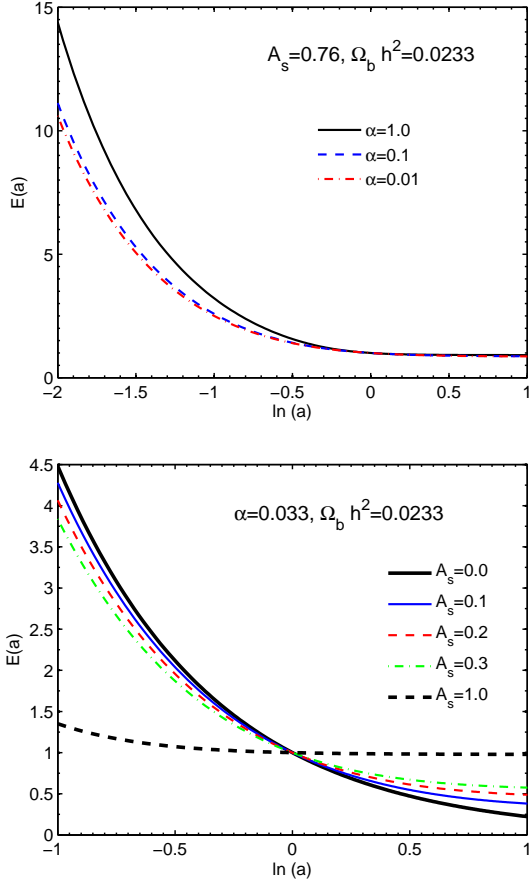


**Fig. 3** Cosmological evolution of normalized Hubble parameter as a function of logarithmic scale factor  $x = \ln a$  in GCG model. In upper panel, we choose the observational best fit values:  $A_s = 0.76$  and  $\Omega_b h^2 = 0.0233$  and vary the parameter  $\alpha$  as 1.0, 0.1 and 0.01 corresponding to black solid, blue dashed and red dotted-dashed lines, respectively. The case of  $\alpha = 1.0$  exhibit the SCG model. In lower panel, by fixing  $\alpha = 0.033$ ,  $A_s$  is varied as 0.0, 0.1, 0.2, 0.3 and 1.0 corresponding to black thick solid line, blue solid line, red dashed line, green dotted-dashed line, black thick dashed line, respectively.

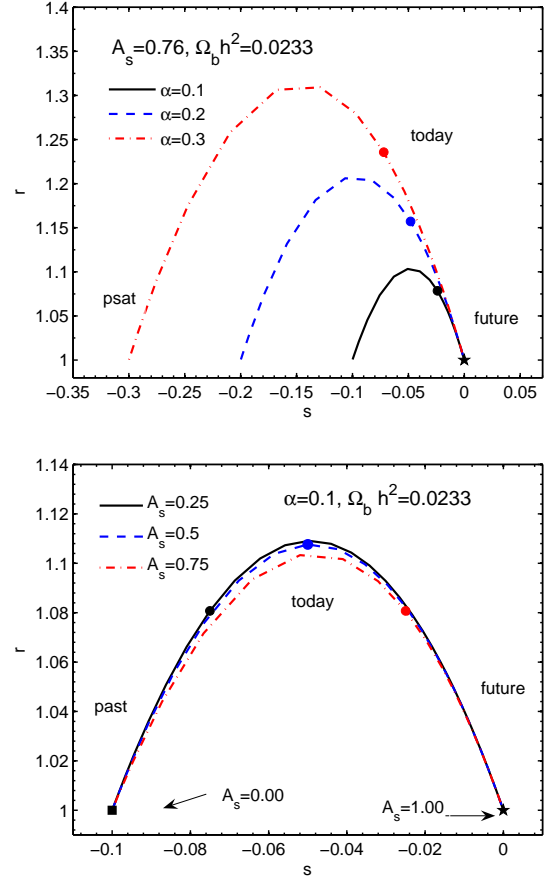


**Fig. 4** An illustrative example for the statefinder diagnostic of GCG model. In upper panel, the evolutionary trajectories in  $s - r$  plane are plotted, by fixing  $A_s = 0.76$  and varying  $\alpha$  as 0.1, 0.2 and 0.3 corresponding to black solid line, blue dashed line and red dotted dashed line, respectively. The circle point on the curves show the today's value of statefinder parameters  $(s_0, r_0)$ . The star symbol indicates the location of standard  $\Lambda$ CDM model in  $s - r$  plane:  $\{s = 0, r = 1\}$ . In lower panel, the evolutionary trajectories are plotted for different illustrative values of  $A_s$ , by fixing  $\alpha = 0.1$ . The case of  $A_s = 0.0$  is related to square symbol located at  $\{s = -0.1, r = 1.0\}$ . Note that  $A_s = 0.0$  represents the CDM model. The case of  $A_s = 1.0$  is exhibited by star symbol at:  $\{s = 0, r = 1.0\}$  which is related to  $\Lambda$ CDM model. The evolutionary trajectories of illustrative cases  $A_s = 0.25$ ,  $A_s = 0.50$  and  $A_s = 0.75$  have been shown by black solid line, blue dashed line and red dotted-dashed line, respectively. Circle point on the curves denotes the today's value  $(s_0, r_0)$  in  $s - r$  plane.



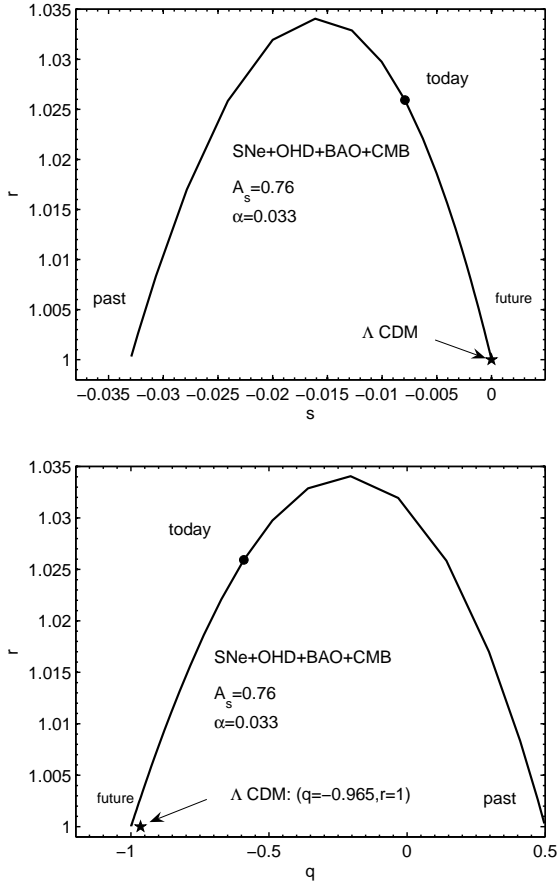


**Fig. 5** The statefinder diagrams  $r(s)$  (upper panel) and  $r(q)$  (lower panel) for GCG model. The evolutionary trajectories are plotted in the light of best fit result of SNe+OHD+BAO+CMB,  $\alpha = 0.033$  and  $A_s = 0.76$ . The circlepoints on the curves show the today's value  $(s_0, r_0)$ , upper panel, and  $(q_0, r_0)$ , lower panel. For comparison, the standard  $\Lambda$ CDM model has been shown by star symbol in these diagrams.

## References

- Alam, U., Sahni, V., Saini, T. D., and Starobinsky, A.A., MNRAS. **344**, 1057 (2003a).
- Alam,U., Sahni, V., Saini, T. D., and Starobinsky, A. A., Mon. Not. Roy. Astron. Soc. **344**, 1057 (2003b) [astro-ph/0303009].
- Allen, S. W., et al., Mon. Not. Roy. Astron. Soc. **353**, 457 (2004).
- Allen, S. W., Rapetti, D. A., Schmidt, R. W., Ebeling, H., Morris, R. G. and Fabian, A. C., Mon. Not. Roy. Astron. Soc. **383** 879 (2008).
- Bilic, N., Tupper, G.B., Viollier, R.D., Phys. Lett. B **535**, 17 (2002);  
Bilic, N., Tupper, G.B., Viollier, R.D., astro-ph/0207423.
- Bento, M. C., Bertolami, O. and Sen, A. A., Phys. Rev. D **66**, 043507 (2002), [arXiv:gr-qc/0202064].
- Bento, M.C., Bertolami, O., Sen, A.A., Phys. Lett. B **575** (2003) 172.
- M. Bordemann, J. Hoppe, Phys. Lett. B 317 (1993) 315;  
J.C. Fabris, S.V.B. Gonsalves, P.E. de Souza, Gen. Relativ. Gravit. **34**, 53 (2002) .
- Boisseau, B., Esposito-Farese, G. , Polarski, D. and Starobinsky, A. A. , 2000 Phys. Rev. Lett. 85 2236.
- Bosma, A. 1981, Astron. J. **86**, 1825.
- Copeland, E. J., Sami, M., Tsujikawa, S., Int. J. Mod. Phys. D **15**, 1753 (2006).
- Caldwell, R. R., Phys. Lett. B **545**, 23 (2002);  
S. Nojiri, S.D. Odintsov, Phys. Lett. B **562**, 147 (2003);  
S. Nojiri, S.D. Odintsov, Phys. Lett. B **565**, 1 (2003).
- Chiba, T., Okabe, T., Yamaguchi, M., Phys. Rev. D **62**, 023511(2000);  
C. Armendariz-Picon, V. Mukhanov, P.J. Steinhardt, Phys. Rev. Lett. **85**, 4438 (2000);  
C. Armendariz-Picon, V. Mukhanov, P.J. Steinhardt, Phys. Rev. D **63**, 103510 (2001).
- Cohen, A., Kaplan, D., Nelson, A., Phys. Rev. Lett. **82**, 4971 (1999);  
P. Horava, D.Minic, Phys. Rev. Lett. **85**, 1610 (2000);  
S. Thomas, Phys. Rev. Lett. **89**, 081301 (2002);  
M. Li, Phys. Lett. B 603, 1 (2004);  
P. Horava, D. Minic, Phys. Rev. Lett. **509** (2001) 138;  
M. R. Setare, Eur. Phys. J. C **50**, 991,2007;  
M. R. Setare, Phys. Lett. B **644**, 99, 2007;  
M. R. Setare, Phys. Lett. B **642**, 1, 2006.
- Cai, R. G., Phys. Lett. B **657** (2007) 228.
- Chang, B.R., Liu, H.Y., Xu, L.X., Zhang, C.W. and Ping, Y.L., JCAP **0701**, 016 (2007) [astro-ph/0612616].
- Chakraborty, W., Debnath, U. and Chakraborty, S., Grav. Cosmol. **13**, 294, 2007.
- Dvali, G., Gabadadze, G., and Porrati, M., 2000 Phys. Lett. B 485 208; I. Brevik, 2008 Eur. Phys. J. C 56 579.
- Eisenstein, D.J., et al, 2005 *Astrophys. J.* **633**, 560 [arXiv:astro-ph/0501171].
- Elizalde, E., Nojiri, S., Odinstov, S.D., Phys. Rev. D **70**, 043539 (2004);  
S. Nojiri, S.D. Odintsov, S. Tsujikawa, Phys. Rev. D **71**, 063004 (2005);  
A. Anisimov, E. Babichev, A. Vikman, J. Cosmol. Astropart. Phys. **06**, 006 (2005).
- Gorini, V., Kamenshchik, A., and Moschella, U., Phys. Rev. D **67**,063509 (2003).
- Gonzalez-Diaz, P. F., Phys. Rev. D **68** 021303 (R), (2003).
- Gori, V., et al., arXiv:0403062. A. Y. Kamenshchik, et al., Phys. Lett. B **511** (2001) 265.
- Hicken, M. , et al., Astrophys. J. **700** 1097 (2009), [arXiv:astro-ph/0901.4804].
- Jassal, H. K., Bagla, J. S. and Padmanabhan, T.,[astro-ph/0601389];  
T. M. Davis et al., [astro-ph/0701510]; L. Samushia and B. Ratra, arXiv:0803.3775 [astro-ph].
- Kamenshchik, A. , Moschella, U. , Pasquier, V., Phys. Lett. B **511**, 265 (2001);  
M.C. Bento, O. Bertolami, A.A. Sen, Phys. Rev. D **66**, 043507 (2002).
- Khodam-Mohammadi,A., Malekjani, M., Astrophys. & Space Sci. 331, 265 (2010).
- Komatsu, E., et al., Astrophys. J. Suppl. **180** 330 (2009) [arXiv:astro-ph/0803.0547]; J. Dunkley, et al., [arXiv:astro-ph/0803.0586].
- Malekjani, M., Khodam-Mohammadi, A., Int. J. Mod. Phys. D, **19**, 1 (2010). [arXiv:1004.0508].
- Perlmutter, S., et al., Astrophys. J. **517** 565 (1999) [astro-ph/9812133].
- Percival, W.J., et al., arXiv:0907.1660 [astro-ph].
- Riess, A. G., et al., Astron. J. **116** 1009 (1998) [astro-ph/9805201].
- Spiegel, D. N., et al., Astrophys. J. Supp. **148** 175 (2003) [astro-ph/0302209].
- Spiegel, D. N., et al., Astrophys. J. Supp. **170** 377 (2007) [astro-ph/0603449].
- Sen, A., J. High Energy Phys. **04**, 048 (2002);  
T. Padmanabhan, Phys. Rev. D **66**, 021301 (2002);  
T. Padmanabhan, T.R. Choudhury, Phys. Rev. D **66**, 081301 (2002).
- Sahni, V. , Saini, T. D. , Starobinsky, A. A. and Alam, U. , JETP Lett. **77**, 201 (2003).  
Setare, M. R., Zhang, J. , and Zhang, X. , JCAP **0703**, 007 (2007) [gr-qc/0611084].
- Sandvik, H. B., et al., Phys. Rev. D 69 (2004) 123524; R. Bean R et al., Phys. Rev. D **68** (2003) 023515.
- Setare, M. R., Eur. Phys. J. C **52**, 689, 2007;  
M. R. Setare, Phys. Lett. B **648**, 329, 2007.
- Shao, Y., and Gui, Y. , gr-qc/0703111.
- Simon, J. , Verde, L., and Jimenez, R., Phys. Rev. D **71** 123001 (2005) [astro-ph/0412269].
- Tegmark, M., et al., Phys. Rev. D **69** 103501 (2004a) [astro-ph/0310723].
- Tegmark, M., et al., Astrophys. J. **606** 702 (2004b) [astro-ph/0310725].
- Wetterich, C., Nucl. Phys. B **302**, 668 (1988);  
B. Ratra, J. Peebles, Phys. Rev. D **37**, 321 (1988).
- Wei, H., Cai, R. G., Phys. Lett. B **655**, 1(2007).
- Xu, L., Lu, J., JCAP, **1003**, 025, (2010) [arXiv:1004.3344] .
- Zhang, X., We, F. Q., Zhang, J., JCAP, 0601 (2006) 003.
- Zhang, L., Cui, J., Zhang, J., & Zhang, X., Int. J. Mod. Phys. D **19**, 21 (2010).
- Zhang, X. , Phys. Lett. B **611**, 1 (2005a) [astro-ph/0503075].
- Zhang, X. , Int. J. Mod. Phys. D **14**, 1597 (2005b) [astro-ph/0504586].
- Zhang, J., Zhang, X., and Liu, H., arXiv:0705.4145 [astro-ph].
- Zimdahl, W. and Pavon, D., Gen. Rel. Grav. **36**, 1483 (2004) [gr-qc/0311067].